



Electrochemical Control of the Magnetic Moment of CrO₂

V. Sivakumar,^a C. A. Ross,^{a,*} N. Yabuuchi,^{b,**} Y. Shao-Horn,^{b,*} K. Persson,^a
and G. Ceder^{a,*}

^aDepartment of Materials Science and Engineering and ^bDepartment of Mechanical Engineering,
Massachusetts Institute of Technology, Cambridge, Massachusetts 02139, USA

The magnetic moment of the half-metallic ferromagnetic oxide CrO₂ has been modified via electrochemical lithiation. In the low-Li regime, below about $x = 0.2$ in Li_xCrO₂, a large change in magnetization of $20 \pm 2\%$ per 0.1 Li/formula unit is obtained, in reasonable agreement with a model based on the change in oxidation state of the Cr ions. The change in magnetization is partly reversible, especially for $x \leq 0.1$. The kinetics and reversibility of the process are improved at 60°C, and Li contents up to $x = 0.9$ could be inserted. At these concentrations the room-temperature moment is reduced to $<5\%$ of its initial value. This decrease is irreversible, due to disruption of the rutile crystal structure of the CrO₂.
© 2008 The Electrochemical Society. [DOI: 10.1149/1.2936261] All rights reserved.

Manuscript submitted January 23, 2008; revised manuscript received March 27, 2008. Available electronically June 13, 2008.

The ability to reversibly manipulate the magnetic properties of materials by external stimuli is of considerable interest in the development of sensors, actuators, and other magnetic devices. In magnetic oxides, the magnetic properties are largely determined by the oxidation state and geometrical arrangement of the magnetic ions, offering the possibility of controlling the magnetic properties electrochemically. For example, the insertion of Li⁺, as occurs during the discharge cycle of a lithium battery, can lead to the reduction of metal cations and a change in magnetic moment. To date, there has been little study of the effects of electrochemical lithiation on the magnetic properties of chromium dioxide. In this work, reversible changes in the magnetization of CrO₂ upon electrochemical cycling have been investigated and related to a model based on the oxidation state of the cations.

CrO₂ is an interesting material because it is the only known stoichiometric binary oxide that is also a ferromagnetic metal.¹⁻⁸ Most transition metal oxides are either antiferromagnetic insulators or ferrimagnets, but CrO₂ possesses a curious mix of electronic conductivity and ferromagnetism³ because the Cr d-bands are divided into two subbands. The first subband is a weakly interacting localized d-state below the Fermi level. These d-states provide the local atomic moments.³ The other band is a hybridized d-band close to the Fermi level which provides metallicity. This makes CrO₂ a half-metal, with a spin polarization (measured by Andreev reflectometry) in the range 80–97% at temperatures close to 1 K.^{1,4-6} Additionally, the presence of room-temperature magnetism in CrO₂ is a desirable property; the Curie temperature is 392 K. CrO₂ crystallizes in the tetragonal rutile crystal structure (space group *P4₂/mnm*, $c/a = 0.6596$) in which half of the octahedral sites are occupied by Cr⁴⁺ ions (Fig. 1).^{9,10} The Cr⁴⁺ ions form a set of edge-sharing octahedra along the *c*-axis and a set of corner-sharing octahedra along the *a*- and *b*-axes. However, CrO₂ is metastable under ambient conditions and transforms into antiferromagnetic Cr₂O₃. It has been successfully grown as a good-quality thin film via chemical vapor deposition.⁶ Historically, CrO₂ has been used in particulate magnetic recording tapes, and also as an oxidizing agent in various chemical reactions. Presently, it is being examined for applications in spintronics.¹¹⁻¹⁴

Insertion of lithium into CrO₂ produces compounds of formula Li_xCrO₂. In its most stable crystal structure at $x = 1$, LiCrO₂ is a Heisenberg antiferromagnet with a Néel temperature of 62 K.¹⁵ In general, LiMO₂ compounds, where M is a transition metal, have a layered structure in which the Li and M ions occupy octahedral sites within a face-centered-cubic (fcc) oxygen lattice.^{16,17} In LiCrO₂ the Cr³⁺ ions occupy points on a two-dimensional (2D) triangular lattice

separated by sheets of lithium and oxygen.¹⁸ LiCrO₂ is isostructural with LiNiO₂, in which Li and Ni are segregated into layers perpendicular to the $\langle 111 \rangle$ direction, and there is a small distortion of the fcc lattice.¹⁹ The LiCrO₂ compound is therefore a rhombohedrally stacked, 2D triangular lattice antiferromagnet, with frustrated antiferromagnetic ground state magnetic order. There has been little work on lithium deintercalation and intercalation in LiCrO₂.²⁰ Deintercalation in Li_xCrO₂ was found to be possible only between $x = 0.8$ and 1.0, and the reversibility was extremely poor.²¹

Experiments on lithium intercalation into CrO₂ have demonstrated a higher capacity (charge storage) in amorphous CrO₂ compared to crystalline CrO₂ (150 and <50 mAh/g, respectively),^{22,23} but there has been no report on the effects of Li content on magnetic properties. One of the key parameters determining the kinetics and reversibility of electrochemical Li insertion in CrO₂ is the diffusivity of the Li ions. While CrO₂ has not been studied in detail, more information is available on TiO₂ in the rutile structure.²⁴⁻²⁸ The TiO₂ rutile structure provides a highly anisotropic framework for diffusion of Li ions, with the diffusion coefficient being at least 5 orders of magnitude greater in the *c*-direction compared to the *a*- and *b*-directions.^{25,26} In TiO₂, inserted lithium ions are expected to occupy octahedrally coordinated sites, which are favored by approximately 0.7 eV over tetrahedral sites.²⁴ It is believed that the limited diffusivity in the *ab* planes restricts the capacity of rutile for Li insertion^{24,26} at room temperature. As the Li content increases and the tetravalent ions are reduced into larger trivalent ions, the lattice expands in the *ab* plane and this enhances the diffusion along the *c*-axis.^{26,27} However, this may not necessarily improve the overall kinetics because the *ab* diffusion is slow.²⁶ Larger Li contents have also been introduced at higher temperatures, for example, 1 mol of Li per formula unit of TiO₂ at 120°C.²⁸

This prior work suggests that the electrochemical Li-ion insertion process may be useful for creating large and reversible changes in the magnetic moment of CrO₂. In this article, the effect of Li insertion on the magnetic properties of CrO₂ powder is investigated and correlated with structural changes. Of particular interest is the extent of reversibility of both the electrochemical behavior and the magnetic properties. Electrochemical reversibility is found to be considerably greater at 60°C as compared to room-temperature cycling. The magnetic moment of the CrO₂ can be varied between its bulk moment and approximately zero magnetization by Li insertion, offering the possibility of using this material in programmable magnetic devices. The results have been related to a model based on the reduction of the Cr⁴⁺ ions to Cr³⁺ as lithiation proceeds.

Experimental

Details of the preparation of positive electrodes (cathodes) and electrochemical schedules can be found in Ref. 29 and 30. Electrochemical cells (type TJ-AC, Tomcell Co., Ltd., Japan) were used for electrochemical measurements. Needle-shaped particles of CrO₂

* Electrochemical Society Active Member.

** Electrochemical Society Student Member.

^z E-mail: caross@mit.edu

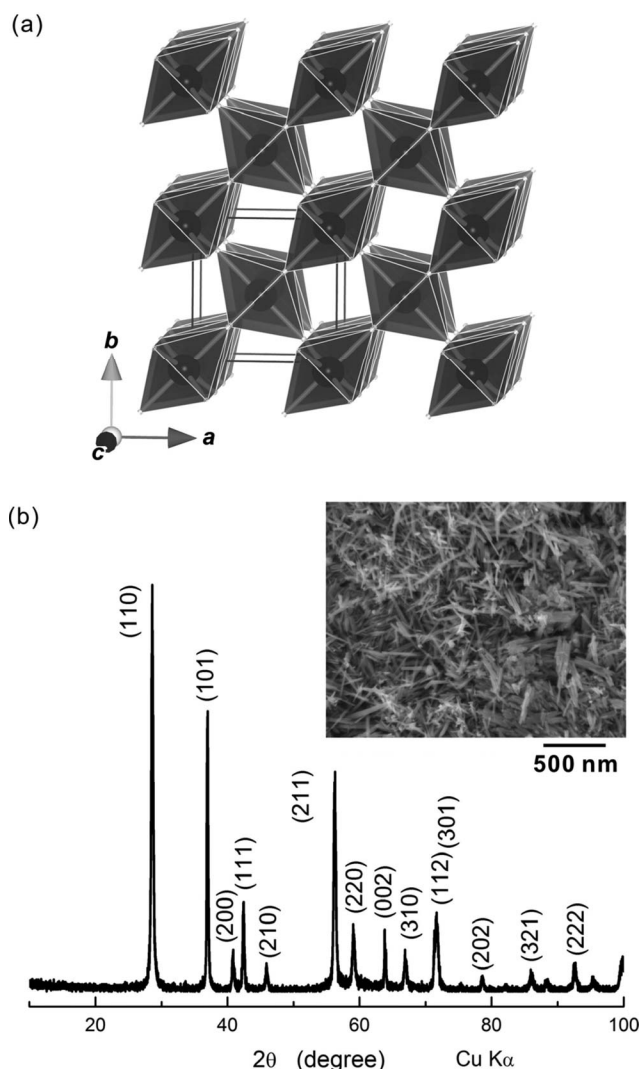


Figure 1. (a) Crystal structure of CrO_2 . (b) XRD pattern of pristine CrO_2 sample. Inset: Scanning electron micrograph of starting CrO_2 sample.

(DuPont Magtrieve) with approximate dimensions of 550×45 nm estimated from a scanning electron micrograph (Fig. 1) were used to make the composite cathodes, which contained a mixture of CrO_2 /Super-P carbon/polyvinylidene difluoride with a weight ratio of 80:10:10. The mixture was cast onto a 20 μm thick aluminum substrate, forming a layer either 79 ± 1.5 or 159 ± 2 μm thick. The substrates were cut into disks and formed into cells with a Li metal anode and 1 M LiPF_6 dissolved in ethylene carbonate/dimethyl carbonate electrolyte. The current applied to the cells was 3.2 mA per gram of CrO_2 , corresponding to the insertion of 0.01 mol of lithium ions per formula unit of CrO_2 every hour. The applied voltage was kept below 4.5 V to avoid electrolyte decomposition and above 0.9 V to avoid reaction with the carbon and binder materials.

The cells were characterized magnetically before and after electrochemical cycling using a vibrating sample magnetometer. The bulk magnetization M_s of the starting CrO_2 powders was 90 emu/g at 10 kOe. CrO_2 powders are difficult to saturate, and a size-dependent magnetization has been reported,³¹ but our value for M_s agrees well with reported values. A high-field paramagnetic slope ($3\text{--}11 \times 10^{-6}$ emu/Oe) observed in the hysteresis curves of the cathodes above 6 kOe that originated from the additives and the aluminum substrate was subtracted from the measurements. This

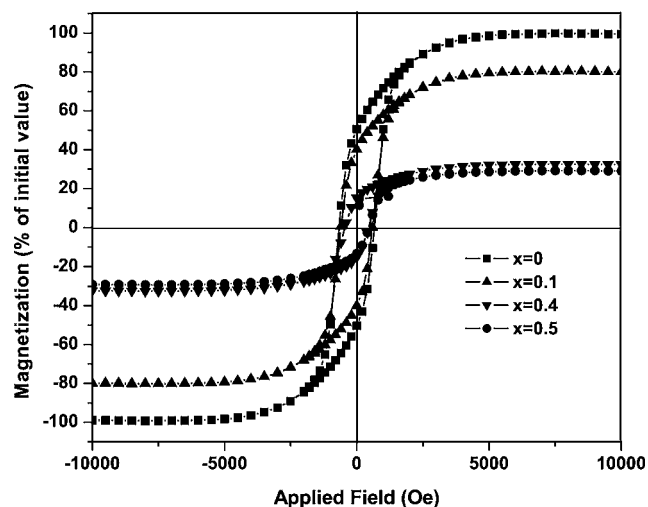


Figure 2. Magnetic hysteresis loops for Li_xCrO_2 with different Li contents x normalized to the magnetization of pristine CrO_2 .

slope subtraction procedure had only a small effect (~ 3 to 4%) on the calculated change in saturation magnetization caused by lithiation.

X-ray diffraction (XRD) of opened cells was carried out in $\theta\text{--}2\theta$ geometry using a diffractometer with $\text{Cu K}\alpha$ radiation. The starting powders contain some trace Cr_2O_3 estimated to be $< 1\%$ from the ratio of XRD peak intensities. The CrO_2 phase may decompose upon exposure to the atmosphere because it is metastable at ambient conditions.³² This was evident in some samples that were exposed to the atmosphere for a prolonged period after overnight vacuum drying at 120°C , in which XRD peaks corresponding to the orthorhombic oxyhydroxide $\text{CrO}(\text{OH})$ phase were found. In order to avoid unwanted reactions, the cathodes were stored and assembled into coin cells inside a glove box prior to the experiments.

Results and Discussion

Electrochemical insertion of Li into CrO_2 at room temperature.— Room-temperature lithiation of CrO_2 led to a decrease in the saturation magnetization of up to 70% (Fig. 2). A maximum of 0.5 mol Li per formula unit of CrO_2 ($x = 0.5$) could be inserted at room temperature during the electrochemical discharge process. The changes in magnetic moment correlate with structural changes apparent from XRD measurements. The CrO_2 (101) rutile-structure peak broadens for $x = 0.1$, and shoulder peaks appear at lower angles for $x = 0.4$ and 0.5 (Fig. 3). This suggests an inhomogeneous

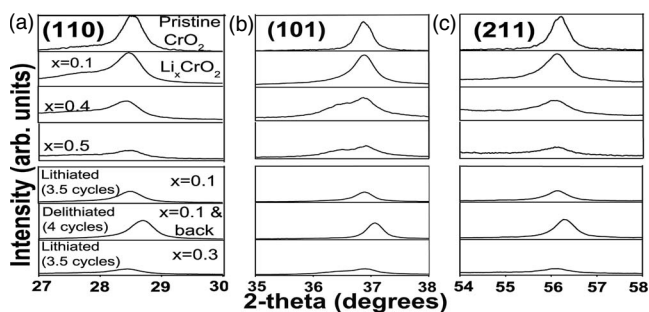


Figure 3. Upper panels: Comparison of (a) (110), (b) (101), and (c) (211) X-ray peaks for samples discharged to different lithium contents $x = 0.1, 0.4$, and 0.5 at 20°C , compared to the peak from the pristine CrO_2 sample. All peaks are shown with the same vertical scale. Lower panels: (a) (110), (b) (101), and (c) (211) peaks for samples after several discharge-charge cycles. All peaks are shown at the same scale as the peaks in the pristine sample.

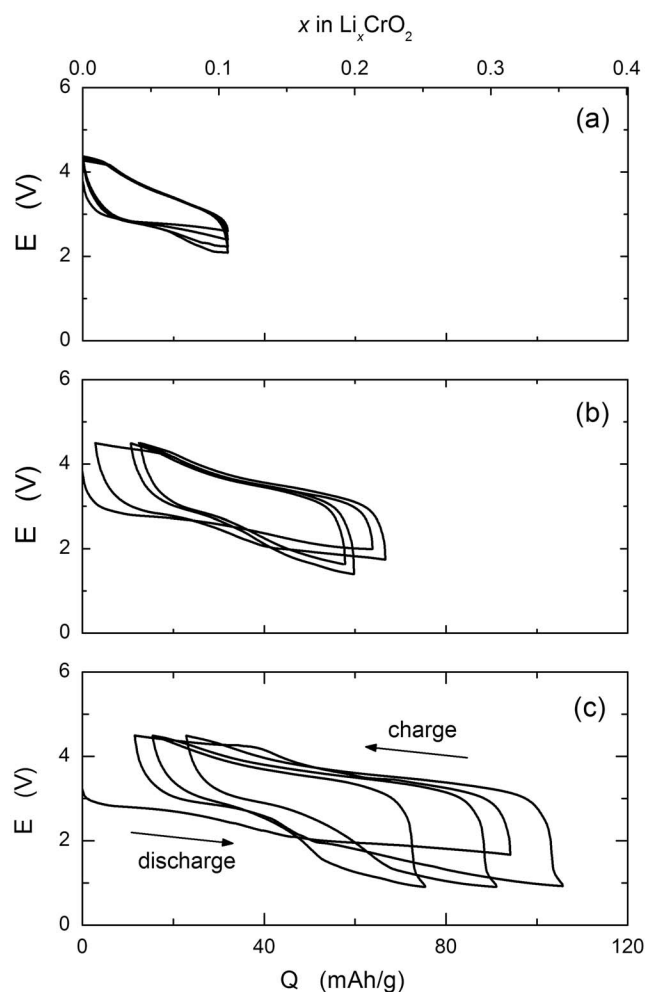


Figure 4. Charge and discharge cycles of CrO_2 samples at a current of 3.2 mA/g at room temperature showing the variation of cell voltage E with charge flow Q : (a) $x = 0.1$, (b) $x = 0.2$, and (c) $x = 0.3$, where x represents the maximum Li content inserted into each sample. The samples were cycled four times.

expansion of the rutile lattice as lithiation proceeds. No peaks from the layered LiCrO_2 phase appeared up to $x = 0.5$. Although the highest intensity peak from this compound would be obscured by a broad background peak from the other materials in the electrode, no other peaks from the compound could be identified. Peaks from the disordered rocksalt phase, observed previously upon lithiation of rutile-structured TiO_2 ,³³ were also not observed up to $x = 0.5$. The shoulder peak is thus attributed to a nonferromagnetic Li^+ - and Cr^{3+} -rich rutile phase. This is consistent with a report in the literature on chemical lithiation of CrO_2 at room temperature involving a topochemical reaction mechanism.³⁴

Electrochemical reversibility of Li_xCrO_2 at room temperature.—The reversibility of the Li insertion was examined by discharging samples (inserting Li) up to different values of x and then charging the samples (removing Li) to return to a nominal composition of $x = 0$. This discharge–charge cycle was repeated up to four times. Figure 4 shows the discharge–charge curves for $x = 0.1$, 0.2, and 0.3. The system shows near-perfect electrochemical reversibility at $x = 0.1$, but a decrease in final voltage is observed upon cycling, which suggests that there is some structural degradation. For $x = 0.2$, there is reasonably good electrochemical reversibility. The sample for $x = 0.3$ shows poor electrochemical reversibility and in this case, the discharge capacity is higher than charging capacity.

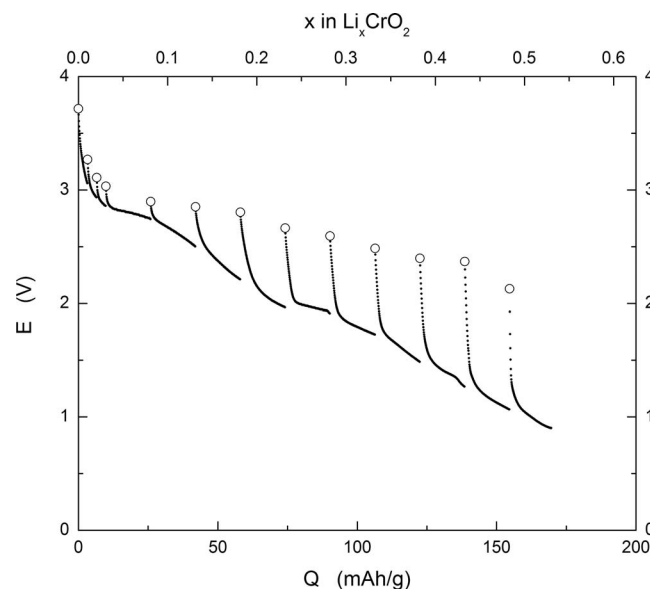


Figure 5. Intermittent charge curves of a CrO_2 sample at a rate of 3.2 mA/g at room temperature. The sample was charged multiple times, each one separated by a 5 h off period. Open circles indicate the OCVs measured after each 5 h current-off period.

The corresponding structural changes are indicated in Fig. 3 (lower panels). As noted above, Li insertion lowers the CrO_2 peak intensity, broadens the peaks, shifts them to lower angles, and introduces additional low-angle shoulders at $x = 0.3$ or higher. Li removal partly reverses these changes and results in an X-ray pattern close to that of the pristine powder, even for $x = 0.3$. For example, a sample discharged to $x = 0.3$ shows a shoulder peak adjacent to the broadened (101) peak, but after cycling four times between $x = 0$ and 0.3 and returning to $x = 0$, the shoulder peak is absent. The peak broadening is not fully reversible, for example, the sample cycled four times to $x = 0.3$ has a full width at half maximum for the (101) peak of 0.49° , compared to 0.33° for the pristine powder and 0.84° for the discharged state. These results suggest that Li insertion creates some irreversible inhomogeneous strain in the lattice. Furthermore, the a -axis lattice parameter, as calculated from the shoulder peak observed for $\text{Li}_{0.1}\text{CrO}_2$ (110), is ~ 4.55 Å. This is 3% longer than the a -axis lattice parameter of the pristine CrO_2 phase. This expansion is consistent with the 9.5% increase observed for the a -axis lattice parameter in $\text{Li}_{0.8}\text{CrO}_2$ prepared by chemical lithiation.³⁴ However, the peak broadening observed in our samples makes a more detailed comparison difficult, particularly for higher lithium contents.

Intermittent discharge measurements (Fig. 5) supported the XRD observations. In these measurements, Li insertion is periodically interrupted by zero-current periods of relaxation lasting 5 h each. The open-circuit voltages (OCVs) observed after 5 h of relaxation decrease as a function of x in Li_xCrO_2 with a relatively small polarization (≈ 200 mV) in the low- x limit. Also, a much larger slope in the OCV x -curve was observed for $x < 0.05$ than for higher lithium contents. This is consistent with the existence of a predominantly single phase at low x , as suggested by XRD. The significantly large polarization (≈ 1000 mV) in the region $x > 0.2$ may indicate a change in the nature of the lithiation reaction at higher Li contents.

Figure 6 shows the magnetization as a function of Li content for different numbers of discharge–charge cycles. Even for $x = 0.1$, a single complete discharge–charge cycle leads to a drop in magnetization of 15% (Fig. 7). Although the process is electrochemically reversible up to $x = 0.1$, the magnetization is not reversible to the same extent. A larger drop in magnetization was obtained for three discharge–charge cycles (Fig. 6), indicating that electrochemical cy-

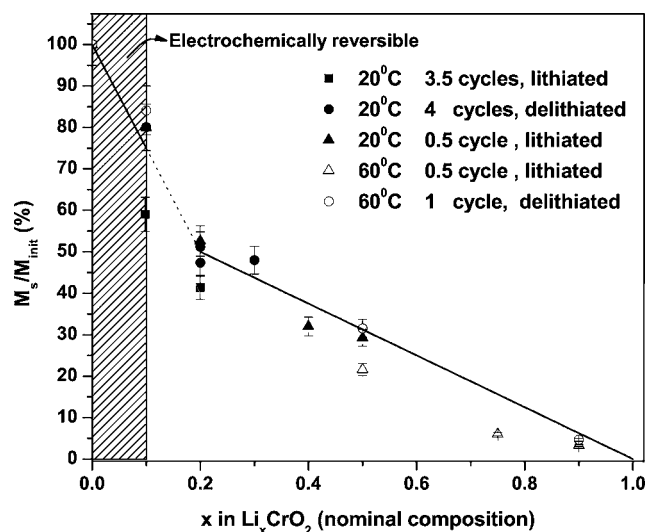


Figure 6. Summary of magnetization measurements of CrO_2 after electrochemical cycling. The samples were subjected to different numbers of discharge–charge cycles and left in the discharged (lithiated) state or the charged (delithiated) state. The solid points indicate room-temperature data while the open points refer to 60°C measurements. For example, “ 20°C 3.5 cycles, lithiated” refers to a sample that has been subjected to three discharge–charge cycles at 20°C , followed by a discharge to leave it at composition x . The shaded area of the graph indicates complete electrochemical reversibility. The line from $x = 0$ to $x = 0.2$ represents the predictions of a model based on the change in the Cr valence state upon lithiation, for samples discharged once (\blacktriangle).

cling leads to progressively higher structural degradation. The irreversibility is more pronounced for higher x , where little of the magnetic moment is recovered upon removing the Li from the structure.

Electrochemical cycling of Li_xCrO_2 at 60°C .— As mentioned above, the kinetics in this system are poor at room temperature, as is evident from the large polarization obtained upon electrochemical cycling. Improvement in the kinetics of lithiation may be expected to increase the amount of lithium that can be inserted and the reversibility of the structural and magnetic changes. To improve the kinetics, samples were subjected to 1–2 electrochemical cycles at 60°C in which Li amounts varying between $x = 0.5$ and 0.9 were

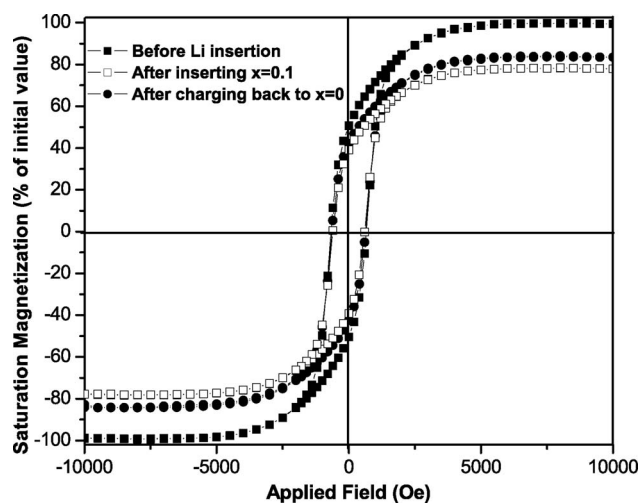


Figure 7. Comparison of magnetic properties before lithiation (\blacksquare), after insertion of $x = 0.1$ mol Li (\square), and after removing Li (charging) back to $x = 0$ (\bullet).

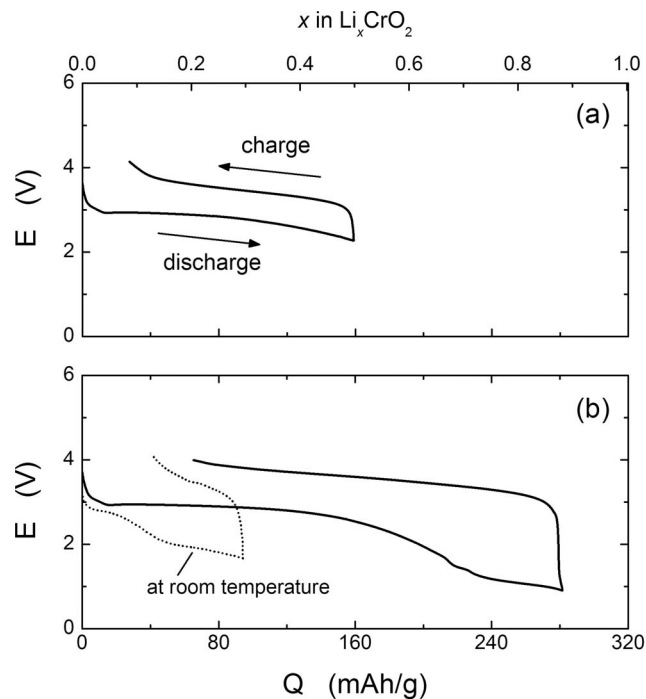


Figure 8. Charge and discharge cycles of CrO_2 samples at a current of 3.2 mA/g at 60°C (solid curve) showing the variation of cell voltage E with charge flow Q : (a) $x = 0.5$ and (b) $x = 0.9$, where x represents the maximum Li content inserted into each sample. The data obtained at room temperature for $x = 0.3$ are shown for comparison in (b) (dotted line).

inserted. Li insertion beyond $x = 0.9$ was limited by the cell, reaching the voltage cutoff of 0.9 V. In Fig. 8, the discharge–charge curves at room temperature and at 60°C are plotted for comparison. There is less polarization at 60°C , implying a reduced kinetic limitation and enabling insertion of more Li than is possible at room temperature.

Structurally, cycling at 60°C also leads to broadening of the (101) peak and development of a shoulder peak at $x = 0.5$ (Fig. 9), which decreases in intensity but does not fully disappear upon charging back to the unlithiated state. At $x = 0.75$ and 0.9 , however, the shoulder peak is retained upon charging back to $x = 0$. The broadening of the (101) peak indicates that there is progressive destruction of long-range order in the rutile lattice, and the broadening becomes increasingly irreversible beyond $x = 0.5$.

The resultant changes in magnetization with Li content at 60°C are superposed on Fig. 6. The magnetization is $<5\%$ of its initial

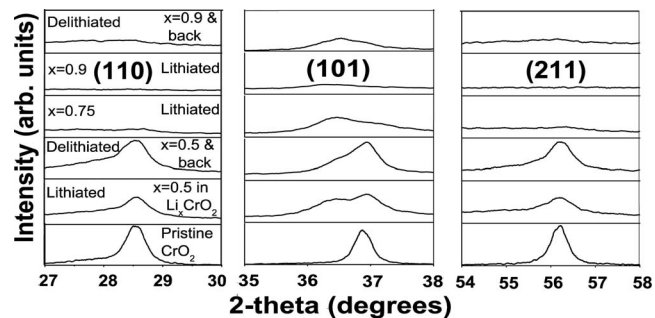


Figure 9. Comparison of the (110) (left), (101) (middle), and (211) (right) rutile peaks for different final charged and discharged states at 60°C . Here the samples were either discharged once (“lithiated”) or discharged and charged back (“delithiated”). All peaks are shown at the same scale as the peaks in the pristine sample.

value when the lithium content reaches $x = 0.75$. However, the reversibility of the change in magnetization is still quite limited, and the electrochemical reversibility evident in the charge–discharge curves, which extends until at least $x = 0.5$ at 60°C , is not matched by the reversibility of the magnetization.

The $M_s(x)$ behavior in the range $x = 0.2$ – 1 is approximately linear (Fig. 6). A possible explanation for this is the presence of two rutile-structure phases, as suggested by the XRD data above $x = 0.2$: one magnetic and the other with no net moment. This is also supported by the intermittent discharge measurement that suggests two different Li insertion mechanisms in the low and intermediate x -regimes (Fig. 5). The change in the voltage across the sample during the 5 h relaxation period is modest (~ 200 mV) for $x < 0.1$ but increases to ~ 1 V for larger x , indicating a change in the kinetics of the Li insertion.

Modeling.—To analyze the effects of Li insertion on the magnetization, we assume that the rutile framework is retained upon lithiation. There are three possible interactions between Cr d -orbitals, namely, e_g – e_g , t_{2g} – t_{2g} , and e_g – t_{2g} . We consider the t_{2g} – t_{2g} interactions alone, because the e_g orbitals are empty. In CrO_2 , the degeneracy of the t_{2g} states is lifted due to tetragonal symmetry. As a result, there exist $d_{yz} + d_{zx}$ and $d_{yz} - d_{zx}$ degenerate excited states above the d_{xy} ground state.⁷ Therefore each Cr^{4+} ion in the lattice has one localized electron in d_{xy} and an itinerant electron that has equal probability of occupying each of the excited states.

The source of the ferromagnetism is the parallel coupling of spins due to hopping of the itinerant electron between neighboring Cr^{4+} (d^2) ions. We assume that insertion of a Li^+ ion leads to reduction of a Cr^{4+} ion (of moment $2\mu_B$) into a Cr^{3+} ion ($3\mu_B$) for charge balance, and that there is no competing charge compensating mechanism, such as the filling of oxygen vacancies. The reduction of Cr^{4+} to Cr^{3+} creates d^2 – d^3 and d^3 – d^3 nearest-neighbor pairs, which leads to antiparallel coupling of spins through superexchange interaction between the t_{2g} orbitals. This is because interactions between half-filled orbitals are antiferromagnetic in nature due to Pauli's exclusion principle and the conservation of spin upon electron transfer.

At low Li concentrations, one can assume that d^2 – d^2 and d^2 – d^3 are the dominant interactions. This gives a ground state wherein the Cr^{4+} ions are coupled parallel to each other and are coupled antiparallel to the small number of Cr^{3+} ions present. Neglecting the parallel coupling between neighboring Cr^{3+} ions, because such pairs would be present in very small concentrations, we expect a decrease in magnetic moment of $5\mu_B$ for each Li^+ ion that is incorporated into the structure. This corresponds to a change in moment of 1629 emu/cm³ at 0 K, or equivalently, a 250% decrease in magnetization, for each mole of Li per formula unit of CrO_2 . A line with this slope is shown in Fig. 6, and is in good agreement with the initial slope of M_s vs Li content x .

The decrease in M_s with x may alternatively be a result of a decrease in Curie temperature with lithiation. To exclude this possibility, the Curie temperature of three lithiated samples was compared with that of the pristine powder. As seen in Fig. 10, the Curie temperature decreases only by about 10°C upon inserting 0.2 mol Li per formula unit, which cannot account for the large changes in room-temperature M_s .

As the Li content increases, d^3 – d^3 and d^3 – d^2 interactions become more dominant, both of which are antiparallel. This suggests that the structure will have little or no net magnetization as it approaches $x = 1$. A loss in moment may also arise from the gradual disruption of the crystalline rutile structure at high x , evident from the XRD data.

Finally, the irreversibility of the magnetic and structural properties, compared with the electrochemical cyclability, is attributed to structural changes or amorphization during the discharge/charge cycles.

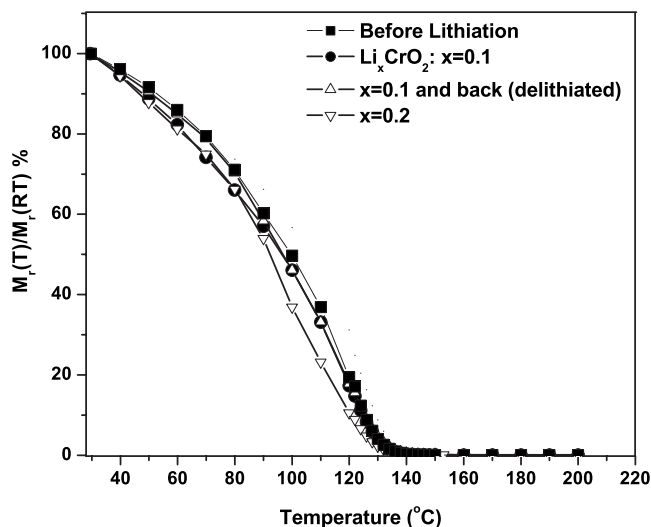


Figure 10. Curie temperature measurements for four CrO_2 samples, pristine (\blacksquare), discharged to $x = 0.1$ (\bullet) or 0.2 (∇), and cycled to $x = 0.1$ and then back to $x = 0$ (\triangle). The figure shows the remanent magnetization after saturation at 8 kOe as a function of temperature.

Conclusion

This study shows that it is possible to create large changes in the magnetization of CrO_2 via electrochemical lithiation at room temperature or at 60°C . In the low-Li regime, below about $x = 0.2$ in Li_xCrO_2 , a large change in magnetization of $20 \pm 2\%$ per 0.1 Li/formula unit is obtained, and is in reasonable agreement with a model (which predicts a 25% change) for the reduction of Cr^{4+} to Cr^{3+} to balance charge as Li^+ is inserted. The change in magnetization is partly reversible, especially at low Li contents (for $x \leq 0.1$). Electrochemically and structurally, the changes appear to be reversible for $x \leq 0.1$, and the partial reversibility of the magnetic changes may indicate the presence of defects such as vacancies in the structure after the discharge–charge cycling, to which the magnetic moment is very sensitive. The kinetics and reversibility of the process are improved at 60°C , and Li contents up to $x = 0.9$ could be inserted into the structure. At these concentrations the room-temperature moment is reduced to $< 5\%$ of its initial value. This decrease is irreversible due to disruption of the rutile crystal structure of the CrO_2 .

Acknowledgments

The authors gratefully acknowledge the Institute for Soldier Nanotechnologies at MIT and the National Science Foundation for financial support, and thank Dr. Gerald F. Dionne of Lincoln Laboratory and Filip Ilievski and David Bono of MIT for useful discussions. We also thank Dr. Hyun-Suk Kim and Dr. Yong Jun Oh of MIT for help with sample preparation.

Massachusetts Institute of Technology assisted in meeting the publication costs of this article.

References

1. J. M. D. Coey and M. Venkatesan, *J. Appl. Phys.*, **91**, 8345 (2002).
2. J. M. D. Coey and S. Sanvito, *J. Phys. D.*, **37**, 988 (2004).
3. B. V. Reddy and S. N. Khanna, *Phys. Rev. Lett.*, **83**, 3170 (1999).
4. R. J. Soulen, Jr., J. M. Byers, M. S. Osofsky, B. Nadgorny, T. Ambrose, S. F. Cheng, P. R. Broussard, C. T. Tanaka, J. Nowak, J. S. Moodera, et al., *Science*, **282**, 85 (1998).
5. W. J. De Sisto, P. R. Broussard, T. F. Ambrose, B. E. Nadgorny, and M. S. Osofsky, *Appl. Phys. Lett.*, **76**, 3789 (2000).
6. Y. Ji, G. J. Strijkers, F. Y. Yang, C. L. Chien, J. M. Byers, A. Anguelouch, G. Xiao, and A. Gupta, *Phys. Rev. Lett.*, **86**, 5585 (2001).
7. P. Schlottmann, *Phys. Rev. B*, **67**, 174419 (2003).
8. J. B. Goodenough, *Prog. Solid State Chem.*, **26**, 359 (1972).
9. M. A. Korotin, V. I. Anisimov, D. I. Khomskii, and G. A. Sawatzky, *Phys. Rev. Lett.*, **80**, 4305 (1998).

10. K. Momma and F. Izumi, *J. Appl. Crystallogr.*, **41**, 653 (2008).
11. I. Zutic, J. Fabian, and S. D. Sarma, *Rev. Mod. Phys.*, **76**, 323 (2004).
12. M. Bibes and A. Barthelemy, *IEEE Trans. Electron Devices*, **54**, 1003 (2007).
13. J. S. Parker, S. M. Watts, P. G. Ivanov, and P. Xiaong, *Phys. Rev. Lett.*, **88**, 196601 (2002).
14. C. M. Fang, G. A. de Wijs, and R. A. de Groot, *J. Appl. Phys.*, **91**, 8340 (2002).
15. M. Suzuki, I. Yamada, H. Kadowaki, and F. Takei, *J. Phys.: Condens. Matter*, **5**, 4225 (1993).
16. T. A. Hewston and B. L. Chamberland, *J. Phys. Chem. Solids*, **48**, 97 (1987).
17. E. J. Wu, P. D. Tepesch, and G. Ceder, *Philos. Mag. B*, **77**, 1039 (1998).
18. A. P. Ramirez, *Annu. Rev. Mater. Sci.*, **24**, 453 (1994).
19. W. Li, J. N. Reimers, and J. R. Dahn, *Phys. Rev. B*, **49**, 826 (1994).
20. S. Madhavi, G. V. Subba Rao, B. V. R. Chowdari, and S. F. Y. Li, *Electrochim. Acta*, **48**, 219 (2002).
21. S. Miyazaki, S. Kikkawa, and M. Koizumi, *Synth. Met.*, **6**, 211 (1983).
22. Y. Takeda, R. Kanno, Y. Tsuji, and O. Yamamoto, *J. Power Sources*, **9**, 325 (1983).
23. J. Kim and A. Manthiram, *J. Electrochem. Soc.*, **144**, 3077 (1997).
24. M. V. Koudriachova, N. M. Harrison, and S. W. de Leeuw, *Phys. Rev. Lett.*, **86**, 1275 (2001).
25. A. Stashans, S. Lunell, and R. Bergström, *Phys. Rev. B*, **53**, 159 (1996).
26. M. V. Koudriachova, N. M. Harrison, and S. W. de Leeuw, *Solid State Ionics*, **157**, 35 (2003).
27. O. W. Johnson, *Phys. Rev.*, **136**, A284 (1964).
28. W. J. Macklin and R. J. Neat, *Solid State Ionics*, **53-56**, 694 (1992).
29. V. Sivakumar, S. Kumar, C. A. Ross, and Y. Shao-Horn, *ECS Trans.*, **2**(8), 1 (2007).
30. V. Sivakumar, S. Kumar, C. A. Ross, and Y. Shao-Horn, *IEEE Trans. Magn.*, **43**, 3121 (2007).
31. X. Zhang, Y. Chen, L. Lu, and Z. Li, *J. Phys. Condens. Matter*, **18**, L559 (2006).
32. M. A. Alario Franco and K. S. W. Sing, *J. Therm. Anal. Calorim.*, **4**, 47 (1972).
33. E. Baudrin, S. Cassaignon, M. Koelsch, J. P. Jolivet, L. Dupont, and J. M. Tarascon, *Electrochem. Commun.*, **9**, 337 (2007).
34. D. W. Murphy, F. J. Di Salvo, J. N. Carides, and J. V. Waszczak, *Mater. Res. Bull.*, **13**, 1395 (1978).